CHAPTER 4 PARAMETRIC STUDY

4.1 Introduction

In general, a bridge is considered to be a system of members like independent beams, slabs, bearings, barrier, substructure, and so on, thus, the overall reliability of the bridge may differ from the reliability of each of its components. The resistance of a bridge depends on loading, redundancies, presence of multiple loads, and the configuration and position of a truck on the bridge. The load carrying capacity of a bridge depends on its geometry (Bishara and Elmir, 1990, Cusens and Pama, 1975; Bangash, 1999; Duanduan and Vivithkeyoonvong, 2001; Balmer and Ramey, 2003), in other words, its number of girders, girder spacing, its connections, and mostly the resistance of its elements. The element resistance is based on the material strength and dimensions. As a result, the component resistance is a random variable as a function of other parameters. These parameters relate to uncertainties associated with dimension and methods of analysis. In order to determine the design $\boldsymbol{M_{LL}}$ (the highest value) for a given number of girders, the bridge deck is designed for HS-44 live load of AASHTO. In this study, the design negative $\boldsymbol{M_{LL}}$ (M_{LL}^{-}) is the largest bending moment that produces compression on the bottom side and tension on the top side of the bridge deck (deck hogging). The design positive $\boldsymbol{M_{LL}}$ (M_{LL}^{+}) is the largest bending moment that produces vice versa effect (deck sagging).

In this Chapter, parameters influencing M_{LL}^{-} and M_{LL}^{+} are evaluated. It has been known for many years that one of the most important parameter involving deck slab design is the spacing of girders (***S***). In general, bridge is normally much longer in ***L*** direction than width of the bridge deck (***W***), and *L/W* ratios of *1.5* or larger are prescribed as a one-way slab (Barker 2007). A typical slab-on-girders deck system actually flexes with much greater curvatures in transverse direction than in longitudinal one. Consequently, the parameter ***S*** will be paid more attention in this study as it always plays a significant role in the deck slab response.

Due to its composite-action behavior, the deck slab trends to deform as one unit with the girder through shear studs. Difference in bridge geometric properties should therefore lead to the variation of slab moments. The presence of truck loads and locations along bridge span where $\boldsymbol{M_{LL}}$ is considered are also influential parameters. Conservatively, the effects of secondary elements (parapet, railing, sidewalk and bearing support) are, however, neglected in this research. Moreover, the phenomenon of

a so-called deck hogging (opposite to a normal deck sagging) is a potential structural deformation that may result in extreme M_{LL}. Notably, this deck hogging has a chance to occur under a real situation at service level of load. Due to the complicated characteristic of the bridge deck discussed above, the approximation of M_{LL} is thus subjected to a challenging topic. Consequently, the present study attempts to carry out the analysis based on those aforementioned parameters so that the most realistic M_{LL} can be evaluated.

4.2 Stiffness Properties of Bridge Decks

Throughout the present parametric study, ESBM modeling technique as discussed in Chapter 3 is used. Poisson's ratios of concrete deck and steel girders are designated to *0.20* and *0.30*, respectively. The value of compressive strength f_c' for cast-in-place concrete slab is also assumed to 35.58 MPa (5.16 ksi) resulting in the slab elastic modulus E_c of 28,270 MPa (4,100 ksi) according to recommendation of ACI 318-08 (ACI, 2008). For steel girders, the magnitude of girder elastic modulus E_g is selected to 199,950 MPa (29,000 ksi). The integer number of the Modula ratio n (E_g/E_c) of 7 is used.

4.2.1 General Girder Stiffness matrix

Prior to the advent of desktop computers, structures were mathematically disassembled to simplify the analysis. FE method does not need this level of simplification lend itself to closed form solution, however the classical principles used still apply as comparison with the numerical method used in this dissertation. All modern structural analysis programs use stiffness methods to model the structures behavior. This involves mapping a member's degrees-of-freedom, through the member stiffness matrix, to the structure degrees-of-freedom creating a global structure stiffness matrix with boundary conditions consistent with the actual structure. Inverting the structure stiffness matrix and multiplying by the load vector yields the structure's displacement vector. From this, all member end forces are obtained. As linear elastic using first order analysis, the general form is:

$$\{d\} = [K]^{-1}\{P\} \tag{4.1}$$

Where

$\{d\}$ = Displacement

$[K]^{-1}$ = Inverted Structure Stiffness Matrix

$\{P\}$ = Load

In the adopted finite element procedure, the contact media at the interface between the top flange of the steel girders and the concrete slab is idealized by a number of linear bar elements with stiffness properties representative of the actual structure at the locations of each element. The load is transferred from the concrete slab to the steel girders through the interface of the provided mechanical connections. It is assumed that the bar element has a rigidity [$\boldsymbol{K}$].

The stiffness general solution procedure consists of formulating an element stiffness matrix. Each element contributes stiffness to the nodes to which it is connected and displaces in a manner which satisfies the force equilibrium and displacement compatibility at the nodes. Normally, the element stiffness matrix of the individual element is first computed and then transformed from the local coordinate system to the global coordinate system. The individual stiffness associated with each nodal point is systematically summed to obtain the total (global) stiffness matrix [$\boldsymbol{K}$] of the structure.

4.2.1.1 Classical T-Beam Stiffness

To determine the spring stiffness of elastic support of slab beam bridges at mid span, it is simply to calculate the elastic spring constant of supporting beam from its deflection. The deflection of the beam ($\boldsymbol{d}$) is determined by the following equation:

$$\boldsymbol{d} = \boldsymbol{L}^3/48\boldsymbol{EI} \tag{4.2}$$

The stiffness [$\boldsymbol{K}$] of elastic support depends on material, geometrical dimensions of the composite section of slab-girder and location along the span in which the stiffness is computed. The moment of inertia is computed from Equivalent Strip Width ($\boldsymbol{SW}$) of AASHTO LRFD (2007). The numerical value of the stiffness [$\boldsymbol{K}$] will be computed as the ratio between applied load and average deflection of the beams at mid-span, left, and right sides of the effective width. At this time, the numerical value of elastic spring constants ($\boldsymbol{K_{GC}}$) of slab-girder is computed as the relation between applied load and deflection of the beam as shown in Figure 4.1 (Tangwongchai, 2003; Tangwongchai and Vivithkeyoonvong, 2003).

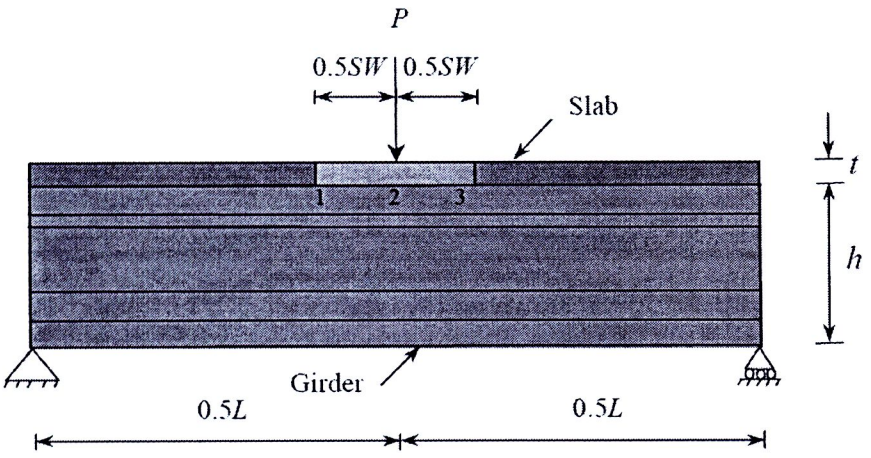

Figure 4.1 Elastic sconstant pring (K_{GC}) of an elastic girder based on ***SW*** width

Therefore, the average K_{GC} can be determined as follows:

$$K_{GC} = 1/d = E_G I_{GC} \left\{ 16/L^3 + 4/\left[SW\left(3L^2 - SW^2\right)\right]\right\} \tag{4.3}$$

Where E_G = modulus of elasticity of the girder, I_{GC} = the moment of inertia of the T-section (T-shape in Figure 2.4), $\boldsymbol{L}$ = span length of the girder, ***SW*** = equivalent strip width of slab by AASHTO LRFD (2007)

Note that AASHTO LRFD Specifications currently provide the contribution of moment of inertia by girder for longitudinal non-composite stiffness (K_g), which is equal to $n(I_g + (e_1+e_2)^2 A_g)$. Therefore, the moment of girder inertia I_g is excluded the effective width of slab. Moreover, AASHTO LRFD Specifications also recommended the *SW* for negative bending (***SW***$^-$) and positive bending (***SW***$^+$). However, these both ***SW***$^-$ and ***SW***$^+$ are not popular in use to compute $\boldsymbol{M_{LL}}$ since it is not convenience compared with AASHTO strip method using Table 4.6.2.1.3-1.

In this dissertation, a set of W33X221 sections is used for the steel girder. K_g of those girders can be readily calculated using Eq. (4.3). Through this approach, the values of K_g are computed by ignoring the deflection of the slab. The magnitudes of K_g^-/P and K_g^+/P due to ***SW***$^-$ and K_g^+/P due to ***SW***$^+$ as well as their stiffness parameters, D_x/D_y and $E_G I_{GC}$ are shown in Table 4.1.

Table 4.1 Stiffness of girders in terms of K_g/P, D_y/D_x and $E_G I_{GC}$

S, m (ft)	K_g/P per unit m						Stiffness Parameter (Plate Theory)	
	L = 15 m (50 ft)		L = 21 m (70 ft)		L = 27 m (90 ft)		D_y/D_x	$E_G I_{gc}/P$
	K_g^-/P	K_g^+/P	K_g^-/P	K_g^+/P	K_g^-/P	K_g^+/P		
1.5 (5 ft)	279	271	120	116	65	63	74	33340
1.8 (6 ft)	279	278	119	119	64	64	65	34970
2.3 (7.5 ft)	278	286	117	121	63	65	55	36930
3 (10 ft)	275	293	114	123	60	66	44	39360
3.6 (12 ft)	273	295	112	124	59	66	38	40830

It should be noted that the physical bridge parameter may be alternatively represented in terms of a bending stiffness parameter of deck slab (D_x) and its composite section (D_y) (Cao and shing 1999) as discussed in section 2.2.7 of Chapter 2. The ratio of D_y/D_x is typically calculated by Equation (2.10) in Chapter 2. It is found that the effect of L on D_y/D_x is neglected in the either Plate Theory or Cao study. Accordingly, the higher value of D_y/D_x in Table 4.1 indicates that the slab will behave much more flexible than the girders. Compared with K_g/P as shown in Table 4.1, it has been also observed that D_y/D_x seems to be less sensitive with S than K_g/P sensitive with L. In particular, K_g/P is relatively constant for each value of L and decrease when L increases. Therefore, K_g/P is considered to be a significant parametric factor than D_y/D_x in the present study.

4.2.2 Effect of Interval Diaphragm Stiffness

The use of various forms of diaphragm is common in bridges. In the case of slab-on-girder type bridges, diaphragms are incorporated mainly to improve the load distribution characteristic of the bridge deck structure. The action of diaphragms influences the lateral distribution of live load and thus affects the sharing of longitudinal moments between the longitudinal girders in the bridge.

In view of effects of interval diaphragm on transverse deck slab moments, the previous study by Jategaonkar and Jaeger (1988) revealed that the for a given loading case, and with bridges having the same number of diaphragms, the total transverse moment remains the same and the distribution of transverse moments is also identical. Moreover, the actual distribution of transverse moment along the span is somewhat different in each case. This distribution depends upon the number of diaphragms and is characterized by local perturbations in proportion to the relative stiffness of diaphragms. This study also concluded that the effects of number of diaphragms is insignificant as it can be proved that, generally, end diaphragms are sufficient to ensure the convergence of the total transverse moment in any specific bridge section.

4.3 General Physical Parameters

Databases of bridges described by some design codes such as OHBDC (1991), BS 5400 (2005), AASHTO (2007) together with a design manual (Heins and Firmage, 1979; Gauvreau, 1990; Hambly, 1991; Iles, 2001; Cook et al., 2002; Brockenbrough and Merritt, 2006) and some noteworthy researches (Firmage and Chiu, 1961; Cheung et al., 1970; Burdette and Goodpasture, 1973; Cao 1996; Chan and Chan, 1999; Tangwongchai and Chucheepsakul 2005) are reviewed to selected the appropriate geometric parameters based on the basis of applicable ranges in bridge design practice. According to the common practice in recent construction and design, geometries of the bridge are normally ranged as follows; a slab thickness (t) of 200 to 225 mm (8 to 9 in), the proportion of L to girder depth H (L/H) of 5 to 30 with the maximum H of 0.91 m (36 in), S of 1.52 m (5 ft) (S_{MIN}) to 3.66 m (12 ft), L of 15 to 27 m (50 to 90 ft). Note that it can be seen in the previous research by Jian J. L. et al (1993) that the slab thickness only plays a minor role.

In addition, if the number of girders is not increased for wider bridges, then the spacing between girders must be increased. This is usually not done in practice, because it leads to thicker concrete slabs and uneconomical design. Therefore, the usual spacing in slab-on-girder bridges is kept in the range of 1.5-2.5 meters.

In order to control the overall deflection, AASHTO provides basic span-to-effective depth ratios that vary according to support conditions (simply supported, continuous, and cantilever). According to AASHTO recommendations, the maximum girder spacing to slab thickness ratio (S/t) and minimum overall depth of composite I-girder ($H+t$) are $L/18$ and $L/25$ (AASHTO 2007), respectively. In this study, construction depths (top of slab to underside of girder) of $L/14.31$ is considered for M_{LL}^{+} and ranging between $L/14.31$ to $L/25.76$ for M_{LL}^{-}. It should be also noted that the most economic solution can be achieved though a fabricated girder with $L/19$.

In general, most of real bridges have the roadway width (w) of 6.10 m to 9.14 m (20 to 30 ft) for double-traffic-lane bridges, zero skew and 0.91 m (3 ft) of the maximum deck overhang. Those values will be used so that the present study conforms the common practice of this bridge design and construction. In general, the minimum number of girders (N_G) in the cross section as compatible with deck design requirements provides the most economical bridge. For example, the Montana Structures Manual (MDT 2004) typically suggests a minimum of four girders in a bridge cross section. However, the use of three girders may be considered on low-volume facilities and the superstructure is not susceptible to impact from overweight vehicles.

In wider roadway bridges with triple traffic lanes, the minimum N_G of 5 and a deck overhang of 1 m (3.28 ft) are typically used. In typical bridge design and construction, the intermediate diaphragms made up of W18x35 steel sections are frequently used and placed at the maximum spacing of 7.62 m (25 ft) along bridge span (AASHTO 2007). In literature, a number of studies was carried out to investigate the influence of intermediate diaphragms on load resistance in slab-on-girder bridges (Sithichaikasem and Gamble 1972, Wong and Gamble 1973). In bridges with a spacing-to-span ratio (S/L) less than 0.05, the presence of diaphragms may lead to more drawback than beneficial (Araujo 2009). Most of those studies have been observed that the improvement of the ultimate capacity due to intermediate diaphragms was not very significant. However, for a practical aspect this diaphragm will be intentionally used throughout this study.

According to information mentioned above, the physical parameters of bridge that produce influential effects on slab moments will be parametrically varied while others will assume to be non-parametric. The definition of the typical bridge deck configuration in normal number of one-lane loading (N_L = 1) is illustrated in Figure 4.2.

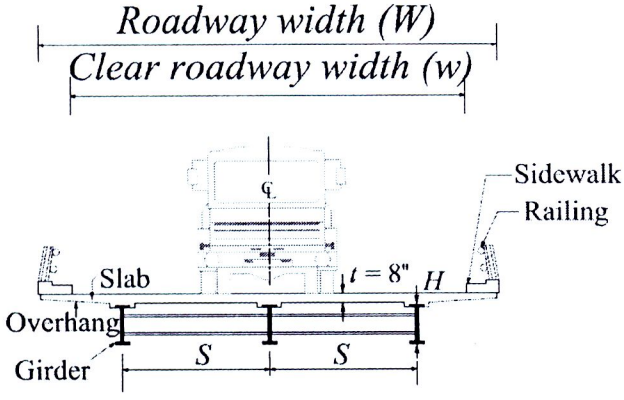

Figure 4.2 Definitions of the typical deck configurations

For various parameters that characterize the geometry of a slab-on-girder bridge, the parametric study based on matter-of-fact bridge characteristics is going to investigate according to the dimensionless values of S/S_{MIN}, W/S and L/H. In general, the possibility of a large number of combinations of S, and N_G makes the design process a trial and error procedure. In the beginning, the width of the bridge deck W is varied according to the variation of S and N_G. For example, the value of 7.92 m (26 ft) will be obtained for W when S and N_G are equal to 1.5 m (5 ft) and 5, respectively. All possible ranges of W together with S and N_G considered in the present study (4.88 m or 16 ft $\leq W \leq$ 10.97 m or 36 ft) are shown in Table 4.2.

Table 4.2 Considered ranges of W ($W = S^*(N_G\text{-}1)$ + Overhangs)

S, m (ft)	N_G	W, m (ft)	W/S
1.52 (5)	3	4.88 (16)	3.2
	4	6.40 (21)	4.2
	5	7.92 (26)	5.2
	6	9.45 (31)	6.2
	7	10.97 (36)	7.2
1.83 (6)	3	5.49 (18)	3
	4	7.32 (24)	4
	5	9.14 (30)	5
	6	10.97 (36)	6
2.29 (7.5)	3	6.40 (21)	2.8
	4	8.69 (28.5)	3.8
	5	10.97 (36)	4.8
3.05 (10)	3	7.92 (26)	2.6
	4	10.97 (36)	3.6
3.66 (12)	3	9.14 (30)	2.5
	4	11 (36)*	3

*without overhangs

In addition, the detail of physical parameters considered in present study can be graphically shown in Figure 4.3. For the simplicity, the author uses the fixed values of t equal to 0.20 m (8 in). Conservatively, the author also uses the constant values H based on the results of a practical range of the bridge design and construction.

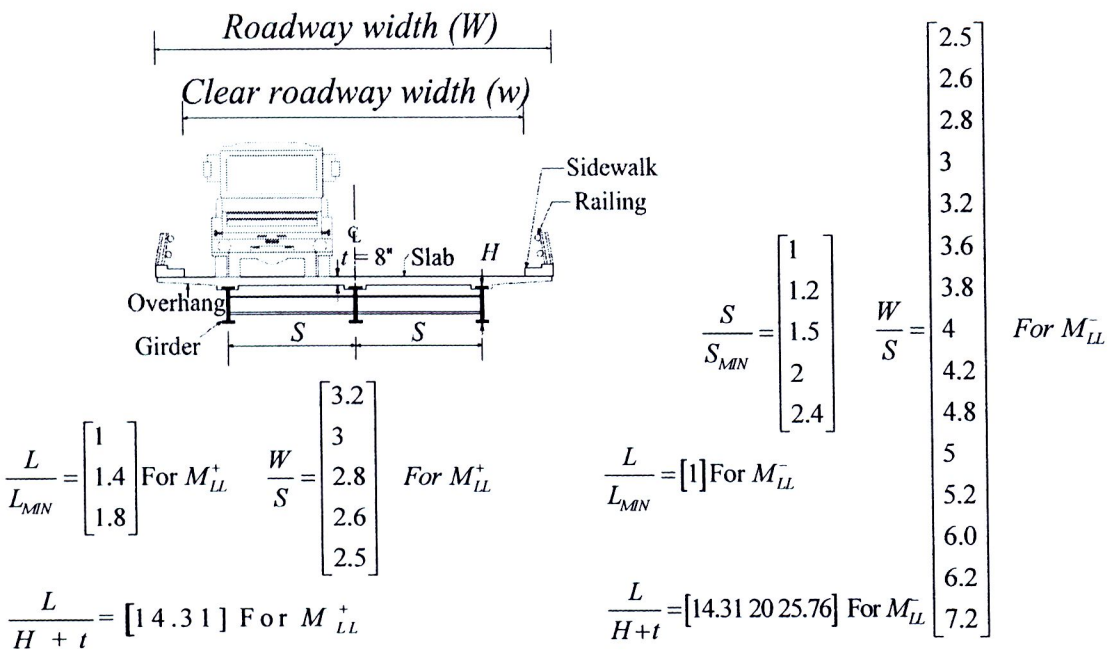

Figure 4.3 Physical parameters considered in this study

4.4 Boundary condition and Loading Location Parameters

The effect of boundary conditions is also considered in this study. There are two cases of boundary conditions, *i.e.* single span with simple supported conditions and double span with continuous supported conditions. The boundary condition parameter (***BC***) is given at this time to stand for support conditions of the bridge. In particular, the bridge with single span and double span will be denoted hereinafter by ***BC*** = 1 and 2, respectively. To take into account for this parameter, pinned-roller restraints are used for the bridge with ***BC*** = 1 and 2. The loading location parameter (y) where M_{LL} is considered is also focused in the present study. Those considered parameters are consequently shown in Figure 4.4.

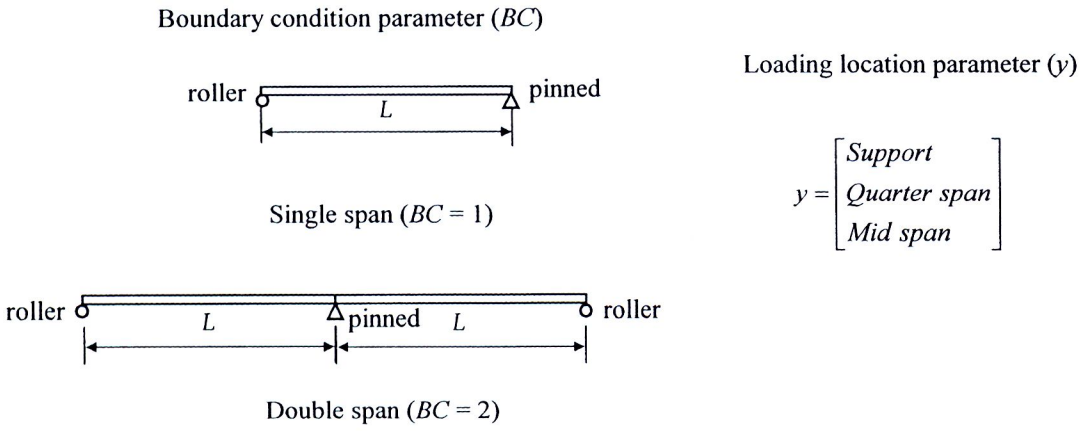

Figure 4.4 Boundary Condition and Loading Location Parameters

4.5 Traffic Characteristic Parameter

In general, the primary design parameter for highway bridges is truck loadings. Truck loading is considered as a transient live load that moves along a bridge. In general, AASHTO provides configuration of a design truck, which is identified as the HS20-44 truck (89 kN or 20 kips) (AASHTO 2007). In this study, the bridge has been analyzed to support the load of this truck. Specifically, the load in the front axis is 35.6 kN (8 kips), 142.3 kN (32 kips) in intermediate axis and 142.3 kN (32 kips) in later axis. To produce loading extreme effect on M_{LL}, the truck can be loaded anyplace on the bridge deck. Therefore, the patterns of truck loading that produce critical M_{LL} should be primarily studied. The parameter of traffic characteristic, which is defined by a presence of loading pattern on the deck (N_L), *i.e.* 1-loaded lane, 2-loaded lane, 2-loaded lane (with deck hogging effect) and 3-loaded lane is investigated herein.

During a real traffic situation, it is considered that an AASHTO design truck can be placed anywhere within a clear width w of a roadway to produce an extreme loading

effect. It is assumed that the wheels of a single axle are spaced at 1.83 m (6 ft) and the minimum distance between the wheels of two side-by-side trucks is set to 1.22 m (4 ft) according to the AASHTO recommendations.

In this study, truck wheel loads are modeled as a patch load distributed over a finite area in FEA models. The tire contact area for an HS20-44 truck is assumed as a rectangle, with a length of 0.51 m (20 in) and a width of 0.25 m (10 in) (AASHTO 2007). To obtain a more accurate estimation of M_{LL}, the tire print loads are enlarged. The contact area of a wheel load given by AASHTO (2007) is enlarged by projecting on the mid-plane of the slab with a distribution angle of 45 degrees (AASHTO 2007) as illustrated in Figure 3.6.

To determine the critical M_{LL}, a single and group of trucks are placed across different transverse locations of the bridge and the trucks are then placed along the longitudinal span by a trial and error procedure. For various values of N_L that characterize the loading pattern, positions of the design truck that produce extreme loading effect on M_{LL} can be examined using FEA influence line analysis. Both critical positions of trucks in transverse and longitudinal traffic directions can be determined as discussed in the following subsection.

4.5.1 Critical N_L in Transverse Traffic Direction

When considered in transverse direction of the bridge deck, the design truck can be placed in different patterns on inside-of-the-way, which may occur during a real traffic situation. It is noted that under different N_L the design truck can be moved anywhere within a clear width w to produce the extreme loading effect. According to AASHTO specifications (Standard, 2002 and LRFD, 2007), it is assumed that the wheels of a single axle are spaced at 1.83 m (6 ft) and the minimum distance between the wheels of two side-by-side trucks is set to 1.22 m (4 ft). Three load patterns, i.e. N_L = 1, 2 and 3 are of interest in this study. To obtain the critical pattern of truck in transverse traffic direction, various cases of loading patterns have been tried on a trial and error basis using FEA. Figs. 4.5 and 4.6 demonstrates the schematic of possible patterns of truck moving laterally on a typical bridge roadway width for the evaluation of M_{LL}^{-} and M_{LL}^{+}, respectively. It is noted that only N_L = 1 is considered for M_{LL}^{+} evaluation. This is due to the fact that for a specific value of S, the critical M_{LL}^{+} is always obtained when the bridge with N_G = 3 is selected as show in Figure 4.5.

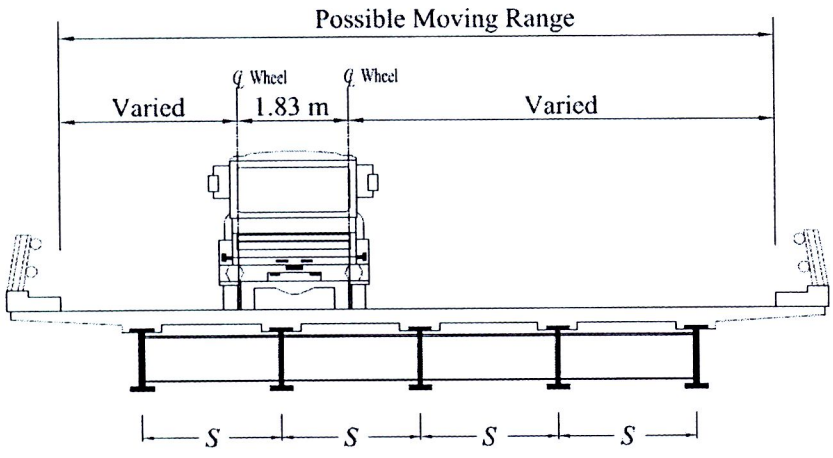

(a) $N_L = 1$

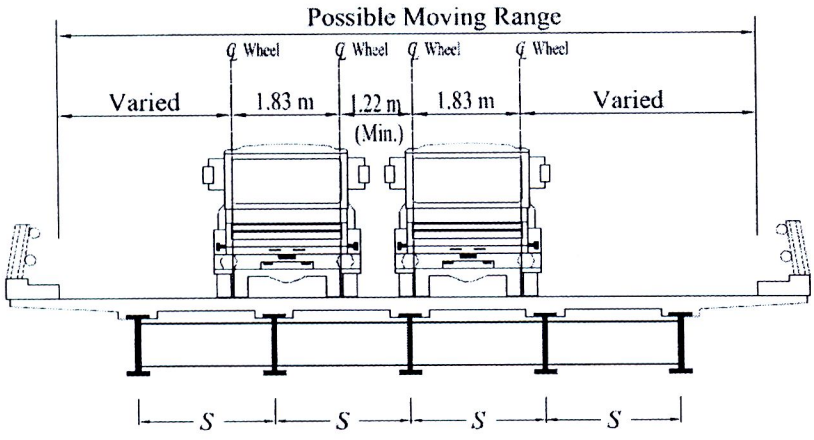

(b) $N_L = 2$

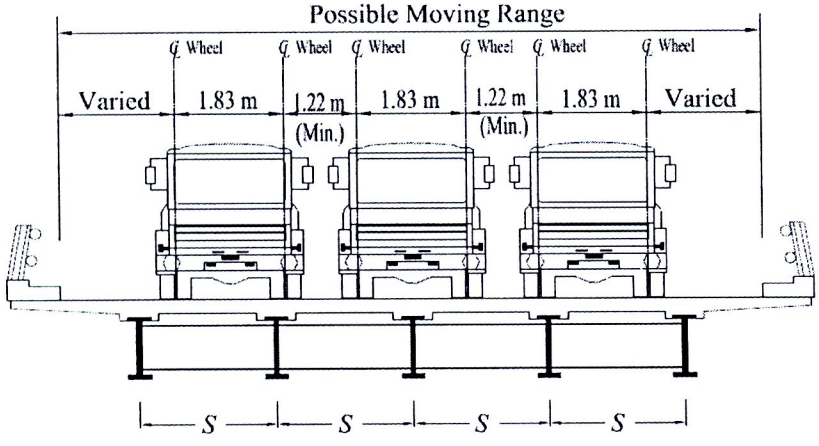

(c) $N_L = 3$

Figure 4.5 Possible patterns of trucks in transverse direction for M_{LL}^{-} evaluation: (a) $N_L = 1$; (b) $N_L = 2$; (c) $N_L = 3$

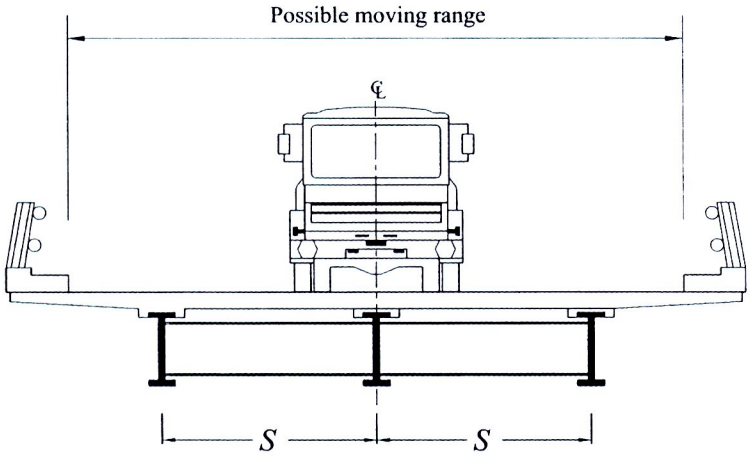

Figure 4.6 Possible patterns of trucks in transverse direction for M_{LL}^{+} evaluation ($N_L = 1$)

Moreover, a specific situation of deck hogging (opposite to a normal deck sagging), which possibly results in critical M_{LL}^{-} is also investigated in this study. In general, the deck hogging only occurs when the trucks are laterally placed on the outermost location of left and right traffic lanes under loading pattern of $N_L = 2$ as illustrated in Figure 4.7.

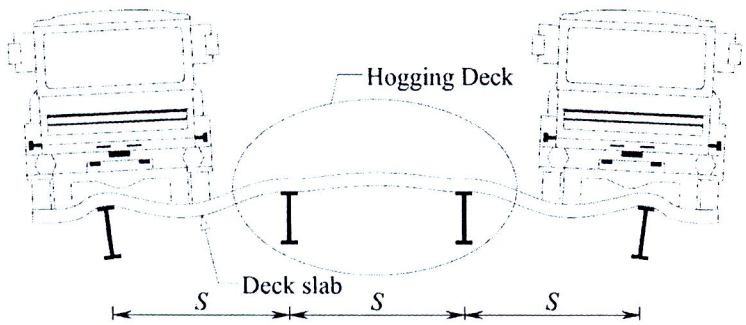

Figure 4.7 Deck hogging due to a specific truck loading pattern under $N_L = 2$

In relation to this loading pattern, a deck hogging can take place when the trucks are loaded at the quarter and mid span only. To observe the deflection of deck cross section at mid span, an investigation is made for a bridge with $S = 3$ m (10 ft) and $N_G = 4$. The deck hogging deflection at the mid span can be numerically proved as shown in Figure 4.9. It has been observed that the magnitude of deflection in case of deck hogging, which is based on $N_L = 2$ is much smaller than that of deck sagging ($N_L = 1$ for this example). Accordingly, the deck hogging tends to produce a certain effect on M_{LL}^{-} only while the deck sagging counterpart should pay a significant role on M_{LL}^{+} in case of $N_L = 1$.

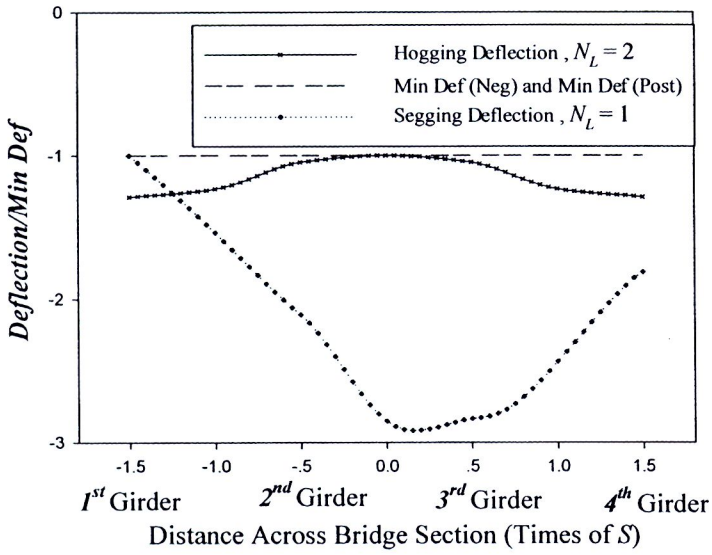

Figure 4.8 Deck hogging and sagging at mid span due to a specific truck loading pattern (bridge with $N_G = 4$)

Based on FEA influence line analysis (trial and error), the variation of loading patterns in transverse traffic direction can be carried out. The critical loading patterns of N_L in transverse traffic direction that produce extreme loading effect on M_{LL} can be therefore monitored at three different locations along bridge span (support, quarter and mid span). It has been observed from the analysis that M_{LL} usually become critical either at the interior or center girders for both odd-number-girder and even-number-girder bridges.

4.5.2 Critical N_L in Longitudinal Traffic Direction

Loading configurations in longitudinal direction, which generate critical M_{LL} at three different locations, *i.e.* y = support, quarter and mid span are subsequently examined. For each of these y, the trucks can be placed with different patterns in transverse traffic direction as discussed in previous subsection. To obtain the critical position of truck wheels in longitudinal direction, the distance between the middle and rear axles V is varied (AASHTO 2007).

4.5.2.1. Design M_{LL}^{-}

Based on FEA influence line analysis, critical M_{LL} usually occurs under either the middle or rear wheels depending on the location of y considered. It is found that at the support, critical M_{LL} occurs only when $L_S = 2$ where the middle wheels (Y_c) with V equal to 4.27 m (14 ft) are placed exactly over the support as shown in Figure 4.9 (a). At the quarter span, critical M_{LL} possibly arises under the rear wheel (Y_2) when V is equal to either 4.27 m (14 ft) in case of $L_S = 1$ with deck hogging or 9.14 m (30 ft) in case of $L_S = 2$ as shown in Figure 4.9 (b). Likewise, there are two loading patterns that produce

critical M_{LL} at mid span. One is for L_S = 1 with deck hogging in which the middle wheels (Y_c) are exactly placed at mid span (V = 4.27 m or 14 ft). The other is for L_S = 2 in which the rear wheels (Y_2) are exactly placed at mid span (V = 9.14 m or 30 ft). Those critical truck patterns are illustrated in Figure 4.9 (c).

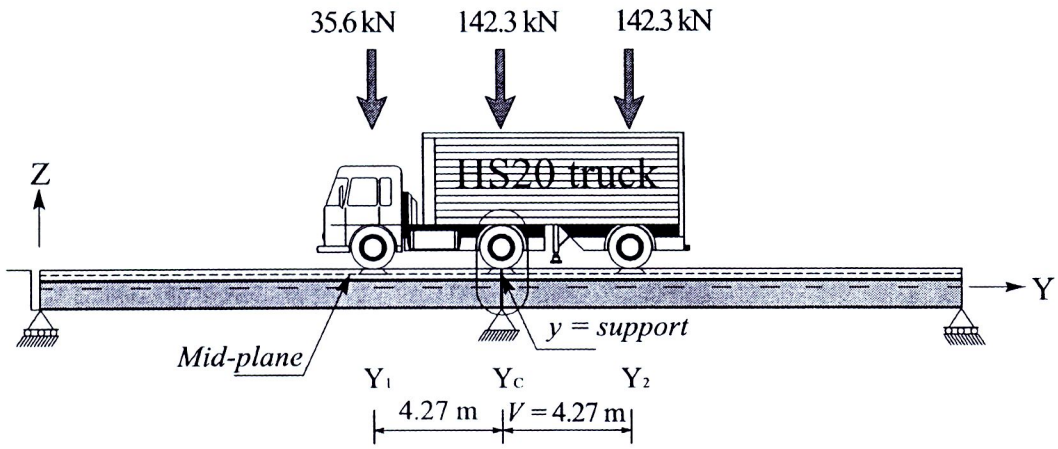

BC = 2; V = 4.27 m (14 ft)

(a) At support

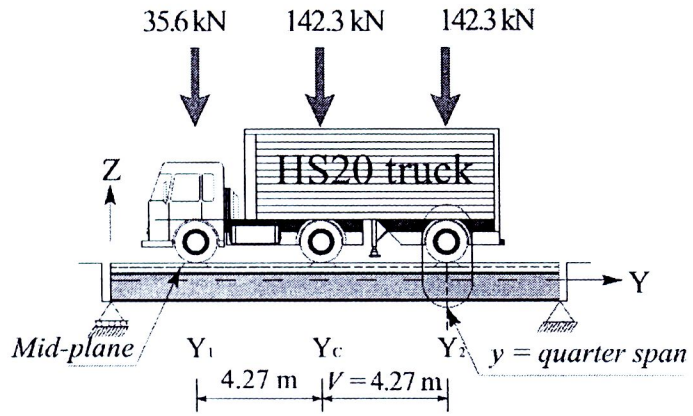

BC = 1 (with deck hogging); V = 4.27 m (14 ft)

(b) At quarter span

Figure 4.9 Critical patterns of design trucks in longitudinal direction for M_{LL}^{-}: (a) At support; (b) At quarter span; (c) At mid span

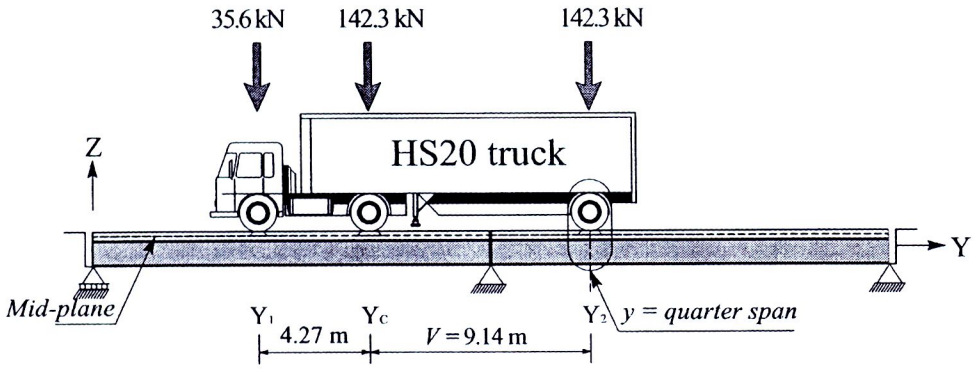

BC = 2; ***V*** = 9.14 m (30 ft)

(b) At quarter span

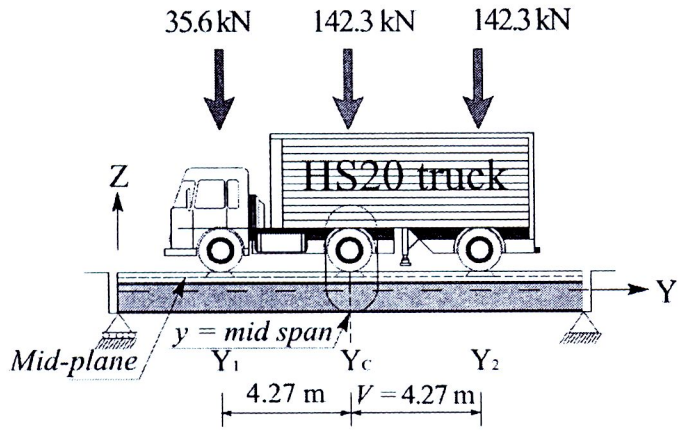

BC = 1 (with deck hogging); ***V*** = 4.27 m (14 ft)

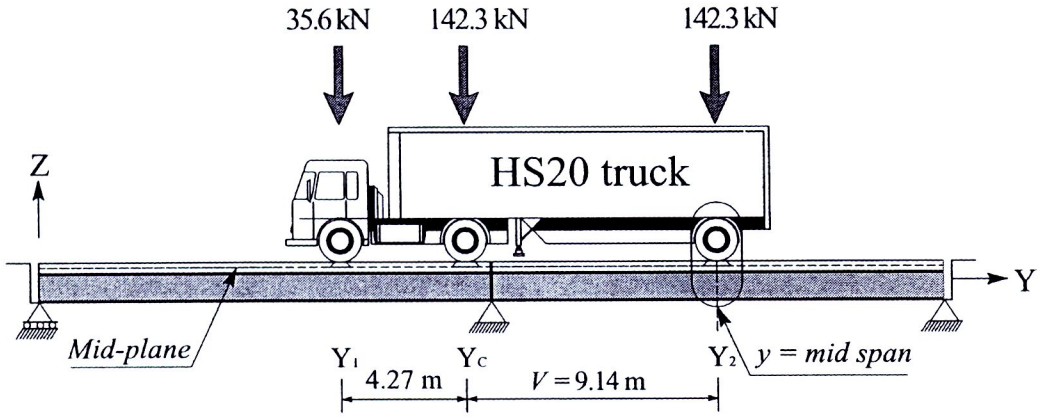

BC = 2; ***V*** = 9.14 m (30 ft)

(c) At mid span

Figure 4.9 (Con't) Critical patterns of design trucks in longitudinal direction for M_{LL}^{-}: (a) At support; (b) At quarter span; (c) At mid span

4.5.1.2 Design M_{LL}^{+}

Unlike the evaluation of M_{LL}^{-}, the patterns of design trucks in longitudinal direction for M_{LL}^{+} evaluation need to consider only one pattern for each y as shown in Figure 4.10. Based on the trial and error analysis, critical M_{LL}^{+} usually occurs under the middle wheel with y = the support and mid span. It has been observed that at the support, critical M_{LL}^{+} occurs only when $BC = 2$ where the middle wheel (Y_c) with V equal to 4.27 m (14 ft) are placed exactly over the support as shown in Figure 4.10 (a). At the quarter span, critical M_{LL}^{+} potentially arises under the rear wheel (Y_2) when V is equal to 4.27 m (14 ft) together with $BC = 1$ as shown in Figure 4.10 (b). Like in case of the support, the same loading pattern for critical M_{LL}^{+} at the mid span can be obtained as illustrated in Figure 4.10 (c).

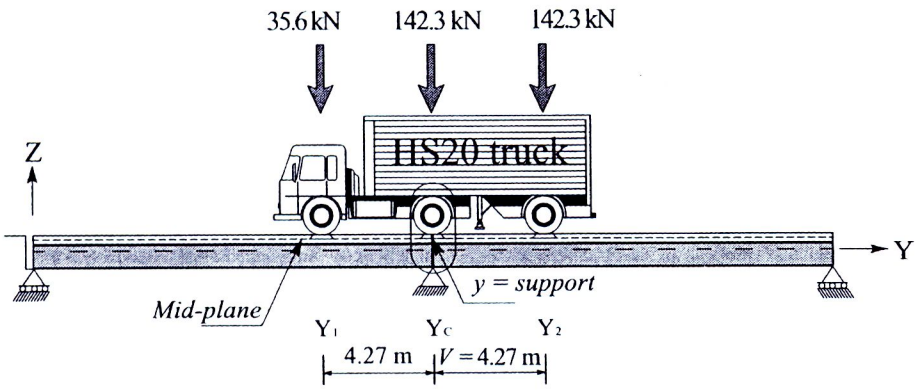

$BC = 2$; $V = 4.27$ m (14 ft)

(a) At support

Figure 4.10 Critical patterns of design trucks in longitudinal direction for M_{LL}^{+}: (a) At support; (b) At quarter span; (c) At mid span

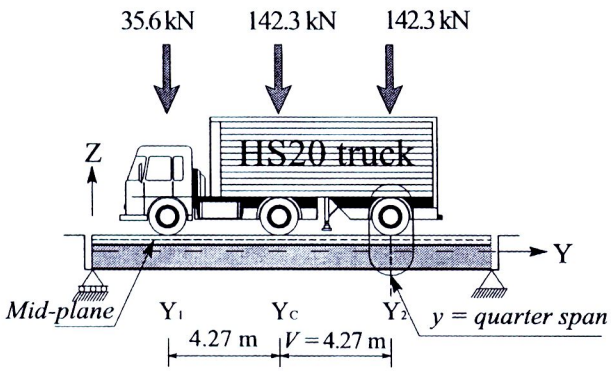

BC = 1; ***V*** = 4.27 m (14 ft)

(b) At quarter span

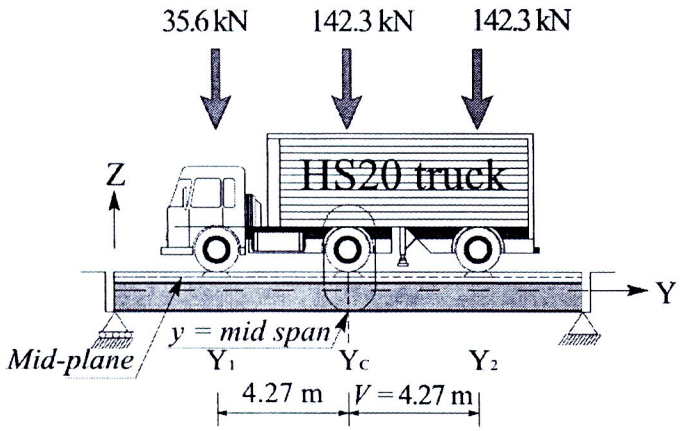

BC = 1; ***V*** = 4.27 m (14 ft)

(c) At mid span

Figure 4.10 (Con't) Critical patterns of design trucks in longitudinal direction for M_{LL}^{+}: (a) At support; (b) At quarter span; (c) At mid span